Conclusion

The present study describes the synthesis, physico-chemical characterization and the *in vivo* antitumor efficacy of the polymer conjugate SP-THP in comparison with the conjugate LP-THP and free THP. More remarkable accumulation of the high-MW conjugate SP-THP (400 kDa, 26nm) in the tumor tissue by EPR effect was observed than in case of LP-THP (39 kDa, 8.2nm). More importantly, SP-THP administration yielded more sustained release of free active THP for a long period of time in the tumor tissue even up to 72h. Thus SP-THP exhibited preferable antitumor effect against both S-180 and AOM/DSS induced colorectal tumor. Even single dose of 15 mg/kg THP equivalent clearly suppressed the tumor growth and prolonged the survival time. These results suggest that large size SP-THP conjugate is superior candidate drug for treatment of various solid tumors.

Acknowledgement

The authors acknowledge support from the Ministry of Health, Labour and Welfare (MLHW) 2007-2013, Japan for Cancer Specialty Grant to Hiroshi Maeda (2011–2014) and from the Matching Fund Subsidy for Private Universities from the Ministry of Education, Culture, Sports, Science and Technology (MECSST), Japan, and Grant Agency of the Czech Republic (grant No. P207/12/J030) and by the project „BIOCEV" (CZ.1.05/1.1.00/02.0109) supported by the European Regional Development Fund.

References

1. Tsukagoshi S. [Pirarubicin (THP-adriamycin)]. *Gan to kagaku ryoho Cancer & chemotherapy* 1988;15: 2819-27.

2. Seymour LW, Ulbrich K, Strohalm J, Kopecek J, Duncan R. The pharmacokinetics of polymer-bound adriamycin. *Biochemical pharmacology* 1990;**39**: 1125-31.

3. Seymour LW, Ulbrich K, Wedge SR, Hume IC, Strohalm J, Duncan R. N-(2-hydroxypropyl)methacrylamide copolymers targeted to the hepatocyte galactose-receptor: pharmacokinetics in DBA2 mice. *Br J Cancer* 1991;**63**: 859-66.

4. Noguchi Y, Wu J, Duncan R, Strohalm J, Ulbrich K, Akaike T, Maeda H. Early phase tumor accumulation of macromolecules: a great difference in clearance rate between tumor and normal tissues. *Jpn J Cancer Res* 1998;**89**: 307-14.

5. Etrych T, Kovar L, Strohalm J, Chytil P, Rihova B, Ulbrich K. Biodegradable star HPMA polymer-drug conjugates: Biodegradability, distribution and anti-tumor efficacy. *J Control Release* 2011;**154**: 241-8.

6. Etrych T, Strohalm J, Chytil P, Cernoch P, Starovoytova L, Pechar M, Ulbrich K. Biodegradable star HPMA polymer conjugates of doxorubicin for passive tumor targeting. *European journal of pharmaceutical sciences : official journal of the European Federation for Pharmaceutical Sciences* 2011;**42**: 527-39.

7. Azori M. Polymeric prodrugs. *Critical reviews in therapeutic drug carrier systems* 1987;4: 39-65.

8. Silva AT, Chung MC, Castro LF, Guido RV, Ferreira EI. Advances in prodrug design. *Mini reviews in medicinal chemistry* 2005;**5**: 893-914.

9. Malugin A, Kopeckova P, Kopecek J. Liberation of doxorubicin from HPMA copolymer conjugate is essential for the induction of cell cycle arrest and nuclear fragmentation in ovarian carcinoma cells. *J Control Release* 2007;**124**: 6-10.

10. Nakamura H, Liao L, Hitaka Y, Tsukigawa K, Subr V, Fang J, Ulbrich K, Maeda H. Micelles of zinc protoporphyrin conjugated to N-(2-hydroxypropyl)methacrylamide (HPMA) copolymer for imaging and light-induced antitumor effects in vivo. *J Control Release* 2013;**165**: 191-8.

11. Hatakeyama H, Akita H, Harashima H. The polyethyleneglycol dilemma: advantage and disadvantage of PEGylation of liposomes for systemic genes and nucleic acids delivery to tumors. *Biological & pharmaceutical bulletin* 2013;**36**: 892-9.

12. Fleige E, Quadir MA, Haag R. Stimuli-responsive polymeric nanocarriers for the controlled transport of active compounds: concepts and applications. *Adv Drug Deliv Rev* 2012;**64**: 866-84.

13. Zamboni WC. Concept and clinical evaluation of carrier-mediated anticancer agents. *Oncologist* 2008;**13**: 248-60.

14. Ulbrich K, Subr V, Strohalm J, Plocova D, Jelinkova M, Rihova B. Polymeric drugs based on conjugates of synthetic and natural macromolecules. I. Synthesis and physico-chemical characterisation. *J Control Release* 2000;**64**: 63-79.

15. Ulbrich K, Etrych T, Chytil P, Jelínková M, Říhová B. Antibody-targeted

polymer-doxorubicin conjugates with pH-controlled activation. *Journal of Drug Targeting* 2004;**12**: 477-89.

16. Etrych T, Jelinkova M, Rihova B, Ulbrich K. New HPMA copolymers containing doxorubicin bound via pH-sensitive linkage: synthesis and preliminary in vitro and in vivo biological properties. *J Control Release* 2001;**73**: 89-102.

17. Nakamura H, Etrych T, Chytil P, Ohkubo M, Fang J, Ulbrich K, Maeda H. Two mechanisms of tumor selective delivery of N-(2-hydroxypropyl)methacrylamide copolymer conjugated with pirarubicin via an acid-cleavable linkage. *J Control Release* 2013.

18. Maeda H. Macromolecular therapeutics in cancer treatment: the EPR effect and beyond. *J Control Release* 2012;**164**: 138-44.

19. Sezaki H, Hashida M. Macromolecule-drug conjugates in targeted cancer chemotherapy. *Critical reviews in therapeutic drug carrier systems* 1984;**1**: 1-38.

20. Ulbrich K, Subr V. Polymeric anticancer drugs with pH-controlled activation. *Adv Drug Deliv Rev* 2004;**56**: 1023-50.

21. Lo CL, Chou MH, Lu PL, Lo IW, Chiang YT, Hung SY, Yang CY, Lin SY, Wey SP, Lo JM, Hsiue GH. The effect of PEG-5K grafting level and particle size on tumor accumulation and cellular uptake. *International journal of pharmaceutics* 2013;**456**: 424-31.

22. Schadlich A, Caysa H, Mueller T, Tenambergen F, Rose C, Gopferich A, Kuntsche J, Mader K. Tumor accumulation of NIR fluorescent PEG-PLA nanoparticles: impact of particle size and human xenograft tumor model. *ACS nano* 2011;**5**: 8710-20.

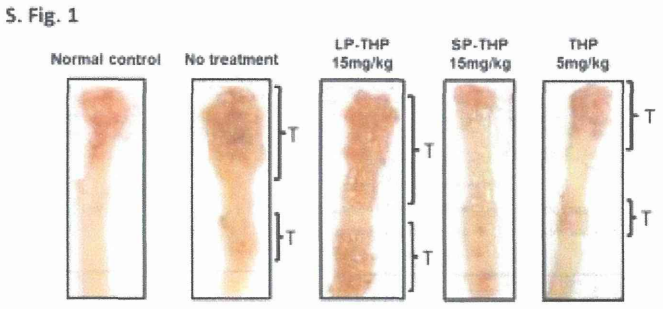

S. Fig.1. Representative images of colon specimen in the each treatment group. T indicates the area of tumor.

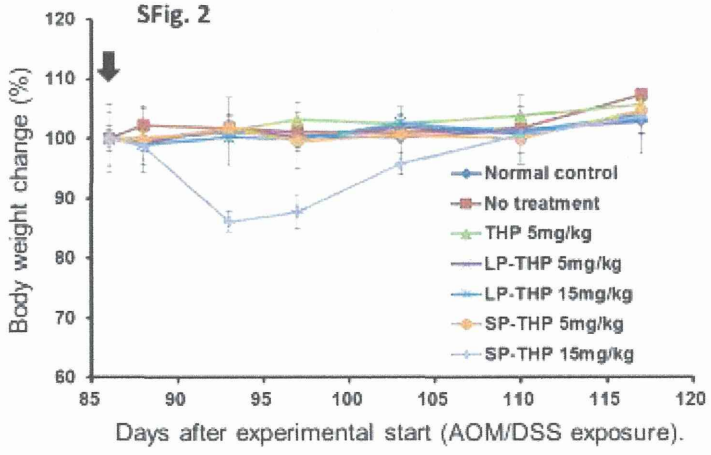

S. Fig. 2. Body weight change after drug administration. Body weights of mice were measured after administration of free THP, SP-THP, or LP-THP at an indicated dosage. Arrows indicates the timing of drug administration. Values are mean ± S.E. (n=5)

S. Fig. 3

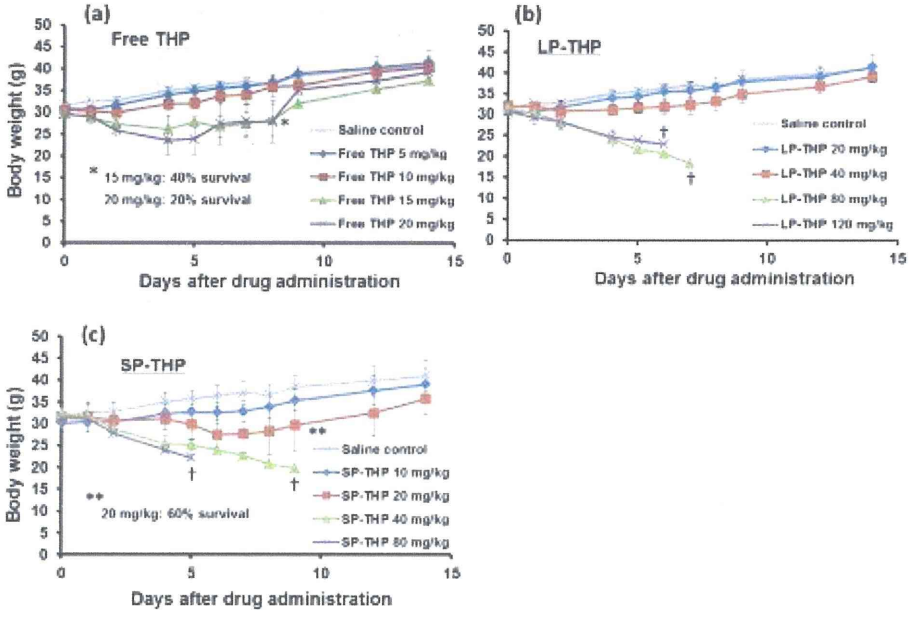

S. Fig. 3. In vivo toxicity of free THP, LP-THP, and SP-THP. Body weights of mice were measured after administration of (a) free THP, (b) LP-THP, or (c) SP-THP at an one indicated dose iv. Values are mean ± S.D. (n=5). † indicates all mice died.

S. Table 1

	Free-THP	LP-THP	SP-THP
LD_{50} (mg/kg, THP equivalent)	14.2	60.0	23.4

S. Table 1. LD_{50} values of polymer THP conjugates in ddY mice (male) of 5 weeks old. LD_{50} values were calculated by method of Reed and Muench.

RESEARCH ARTICLE – *Pharmaceutical Nanotechnology*

Tuning of Poly-*S*-Nitrosated Human Serum Albumin as Superior Antitumor Nanomedicine

YU ISHIMA,[1,2] JUN FANG,[3] ULRICH KRAGH-HANSEN,[4] HONGZHUAN YIN,[3] LONG LIAO,[3] NAOHISA KATAYAMA,[5] HIROSHI WATANABE,[1,2] TOSHIYA KAI,[6] AYAKA SUENAGA,[1] HIROSHI MAEDA,[7] MASAKI OTAGIRI,[1,3,7] TORU MARUYAMA[1,2]

[1]Department of Biopharmaceutics, Graduate School of Pharmaceutical Sciences, Kumamoto University, Kumamoto 862-0973, Japan
[2]Center for Clinical Pharmaceutical Science, Kumamoto University, Kumamoto 862-0973, Japan
[3]Faculty of Pharmaceutical Sciences, Sojo University, Kumamoto 860-0082, Japan
[4]Department of Biomedicine, University of Aarhus, Aarhus CDK-8000, Denmark
[5]Pharmaceutical Research Laboratories, Kusatsu, Shiga 525-0055, Japan
[6]Tohoku Nipro Pharmaceutical Corporation, Kagamiishimachi, Iwasegun, Fukushima 969-0401, Japan
[7]Drug Delivery System Institute, Sojo University, Kumamoto 860-0082, Japan

Received 14 March 2014; revised 23 April 2014; accepted 2 May 2014

Published online in Wiley Online Library (wileyonlinelibrary.com). DOI 10.1002/jps.24020

ABSTRACT: Macromolecules have been developed as carriers of low-molecular-weight drugs in drug delivery systems (DDS) to improve their pharmacokinetic profile or to promote their uptake in tumor tissue via enhanced permeability and retention (EPR) effects. We have previously demonstrated that poly-nitric oxide (NO) conjugated human serum albumin (Poly-SNO-HSA) has the potential to be a DDS carrier capable of accumulating NO in tumors. However, the stability of Poly-SNO-HSA in the circulation has to be improved, and its optimal molecular size for using the EPR effects has to be evaluated. In the present study, we performed two tuning methods for refining Poly-SNO-HSA, namely, pegylation and dimerization. We observed that pegylation enhanced the stability of Poly-SNO-HSA both *in vitro* and *in vivo*, and that dimerization of Poly-SNO-HSA enhanced the antitumor activity via more efficient delivery of NO in Colon 26 tumor-bearing mice. Intriguingly, dimerization resulted in a 10 times higher antitumor activity. These data suggest that pegylation and dimerization of Poly-SNO-HSA are very important tuners to optimize NO stability and accumulation, and thereby effect, in tumors. Thus, polyethylene glycol-Poly-SNO-HSA dimer seems to be a very appealing and safe NO carrier and thereby a strong candidate as an antitumor drug in future development of cancer therapeutics. © 2014 Wiley Periodicals, Inc. and the American Pharmacists Association J Pharm Sci
Keywords: human serum albumin; nitric oxide; drug delivery system; antitumor activity; pegylation; dimerization; cancer; controlled release/delivery; macromolecular drug delivery; nanoparticles

INTRODUCTION

Cancer treatment remains one of the most important clinical challenges. One problem in treating various cancers is the development of multidrug resistance (MDR) by the cancer cells. Various approaches have been tested to overcome MDR such as the use of agents that inhibit P-glycoprotein directly or indirectly through altering the cell membrane. Most of the approaches have shown some success in small animal models but their clinical application has been limited. Because nitric oxide (NO) seems to be able to overcome MDR, and has other promising properties and effects, it has the potential of becoming a useful anticancer therapeutic.[1,2]

Nitric oxide is a free-radical gas involved in diverse biological processes, such as neurotransmission, blood pressure control, inhibition of platelet aggregation, and innate immunity.[3] However, under certain circumstances, NO can be cytotoxic. For example, high concentrations of NO can inhibit tumor cell growth and induce apoptosis.[4,5] Recent studies have revealed that NO is associated not only with apoptosis of cancer cells, but also with inhibition of cancer progression and metastasis, as well as cancer angiogenesis and microenvironment. It also functions as a modulator for chemo/radio/immunotherapy.[6] Despite highly useful properties, the *in vivo* half-life of NO is so short that NO itself cannot be used as a therapeutic agent. Such a short half-life can be overcome using continuous release of NO from a reservoir, such as the *S*-nitrosated form of human serum albumin (HSA).[7–9]

Our previous studies with cell cultures demonstrated that the NO influx from poly-nitric oxide conjugated human serum albumin (Poly-SNO-HSA) via cell surface protein disulfide isomerase is very fast and pronounced and leads to cell death caused by apoptosis. However, the apparent *in vivo* half-life of *S*-nitroso moieties in Poly-SNO-HSA has been estimated to be 18.9 min in tumor-bearing rats, indicating that it is not always a long-acting medicine.[10] Therefore, the release rate of NO from Poly-SNO-HSA needs to be well controlled and prolonged to develop more effective NO delivery systems. Shishido and de Oliveira[11] have shown that the thermal stability of *S*-nitrosothiols is increased in polyethylene glycol (PEG) solution because the cage effect of PEG increased the stability of S–NO bonding. Perhaps, this effect can be applied to construct more useful Poly-SNO-HSA preparations.

In addition to *in vivo* half-life, the problem of drug targeting should be addressed. In this respect, the enhanced permeability

Correspondence to: Toru Maruyama (Telephone: +81-96-371-4150; Fax: +81-96-362-7690; E-mail: tomaru@gpo.kumamoto-u.ac.jp), Masaki Otagiri (Telephone: +81-96-326-3887; Fax: +81-96-326-5048; E-mail: otagirim@ph.sojo-u.ac.jp)

Journal of Pharmaceutical Sciences

and retention (EPR) effect is relevant. This effect is now known to play a major role in the tumor-selective delivery of macromolecular or polymeric drugs, or of so-called nanomedicines including antibodies.[12–14] It is well known that long-circulating liposomes with an average diameter of 100–200 nm accumulate efficiently in tumor tissues.[15] Matsumura and Maeda[16] found that high-molecular-weight (40 kDa or higher), long-circulating macromolecules, as well as various long-circulating nanoparticulate pharmaceutical carriers are capable of spontaneously accumulating in various pathological sites, such as solid tumors and infracted areas. However, recently, Kataoka's group demonstrated that only 30-nm micelles could penetrate poorly permeable pancreatic tumors to achieve an antitumor effect.[17] These data suggest that macromolecular therapeutics with a size of 30 nm could efficiently deliver to even poorly permeable tumors. For testing this possibility, we have designed a HSA dimer, in which the C-terminus of one HSA molecule is linked to the N-terminus of another HSA molecule by the amino acid linker $(GGGGS)_2$, that can be successfully produced by the yeast *Pichia pastoris*. We have previously reported that HSA dimer has a longer circulation time than the monomeric form of HSA, HSA monomer, in rats and mice.[18] Moreover, HSA dimer could have an enhanced accumulation in solid and poorly permeable tumors via the EPR mechanism because of its molecular size of approximately 30 nm (130 kDa). Therefore, it is possible that HSA dimer could be of great clinical use as a new DDS material with a superior plasma retention property (e.g., prolonged plasma half-life) as well as with increased tumor-specific accumulation.

In this study, we performed two tuning methods of pegylation and dimerization of Poly-SNO-HSA. We examined the effect of pegylation on the stability of *S*-nitrosated sites of Poly-SNO-HSA *in vitro* and *in vivo*, and the effect of dimerization of Poly-SNO-HSA on its antitumor activity in Colon 26 (C26) tumor-bearing mice.

MATERIALS AND METHODS

Materials

Human serum albumin and HSA dimer were synthesized using the yeast *Pichia pastoris* (*P. pastoris*) (strain GS115) as previously described,[18] and the proteins were defatted by means of charcoal treatment.[19] Sephadex G-25 desalting column (ϕ 1.6 × 2.5 cm) was obtained from GE Healthcare (Kyoto, Japan). 1,4-dithiothreitol was obtained from Sigma–Aldrich (St. Louis, Missouri). Isopentyl nitrite (IAN) was bought from Wako Chemicals (Osaka, Japan). Diethylenetriaminepentaacetic acid (DTPA) and ethylenediaminetetraacetic acid were purchased from Nacalai Tesque (Kyoto, Japan). $^{111}InCl_3$ was a gift from Nihon Medi-Physics Company, Ltd. (Hyogo, Japan).

Cells and Animals

C26 cells were cultured in RPMI-1640 containing 10% fetal bovine serum (Sanko Junyaku Co, Ltd.,Tokyo, Japan), 100 units/mL penicillin, and 100 μg/mL streptomycin, incubated in a humidified (37°C, 5% CO_2 and 95% air) incubator, grown in 75-cm^2 flasks (Falcon BD) Tokyo, Japan, and passaged when 75% confluency was reached. Male BALB/cAnNCrlCrlj mice (5 weeks old, 17–22 g) were purchased from Charles River Laboratories (Ibaraki, Japan). A C26 solid tumor model was established by subcutaneously implanting 2×10^6 C26 cells into the back of the mice. Other animals, that is, male ddY mice and male Donryu rats, were from Kyudo Inc. (Kumamoto, Japan).

Pegylation and *S*-Nitrosation

To perform the pegylation of HSA, HSA–polyethylene glycol conjugate-5000 (PEG–HSA) was synthesized by reacting activated PEG with HSA in 50 mM borate buffer (pH 9.2) for 24 h at 4°C in the dark to react with available amino acids.[20] The reaction mixture was then washed and concentrated by ultrafiltration against distilled water. The average number of PEG moieties is 4.6 mol PEG/mol HSA, and the molecular weight of the product is estimated to be 90 kDa by using SDS-PAGE (data not shown).

Poly-nitric oxide conjugated human serum albumins were prepared according to a previous report.[4] In brief, terminal sulfhydryl groups were added to HSA, PEG–HSA, and HSA dimer by incubating 0.15 mM HSA, 0.15 mM PEG–HSA or 0.075 mM HSA dimer with 3 mM Traut's Reagent (2-imminothiolane) in 100 mM potassium phosphate buffer containing 0.5 mM DTPA (pH 7.8) for 1 h at 25°C. The resultant modified HSA, PEG–HSA, and HSA dimer was then *S*-nitrosated by 3 h incubation with 15 mM IAN at 25°C. The resulting Poly-SNO-HSA, PEG-Poly-SNO-HSA, or Poly-SNO-HSA dimer was concentrated, exchanged with saline using a PelliconXL filtration device (Millipore Corporation, Billerica, Massachusetts), and the final concentration was adjusted to 2 mM Poly-SNO-HSA, 2 mM PEG-Poly-SNO-HSA, or 1 mM Poly-SNO-HSA dimer. The samples were stored at 80°C until use . The number of NO moieties bound to Poly-SNO-HSA and PEG-Poly-SNO-HSA is 6.7 mol NO/mol protein, whereas the number bound to Poly-SNO-HSA dimer is 13.5 mol NO/mol protein.

Pharmacokinetic Experiments

Poly-nitric oxide conjugated human serum albumin was labeled with ^{111}In by using DTPA anhydride as a bifunctional chelating agent.[21] Labeled Poly-SNO-HSA was injected via the tail vein into male ddY mice (weighing 25–27 g) at a dose of 5 μmol NO/kg. At appropriate times after injection, blood was collected from the vena cava with the mouse under ether anesthesia. Heparin sulfate was used as an anticoagulant, and plasma was obtained from the blood by centrifugation. The radioactivity in each sample was counted using a well-type NaI scintillation counter ARC-2000 (Aloka, Tokyo, Japan). ^{111}In radioactivity concentrations in plasma were normalized as a percentage of the dose injected per milliliter and were analyzed by means of the nonlinear least-squares program MULTI.[22] We also measured the amount of *S*-nitrosated moieties in the plasma samples. That was performed by means of the Saville assay.[23]

Effect of Pegylation on the Stability of S-Nitrosated Sites of Poly-SNO-HSA

For *in vitro* study, Poly-SNO-HSA or PEG-Poly-SNO-HSA at a NO concentration of 100 μM was incubated in mouse blood or plasma at 37°C for different times in the dark. For *in vivo* study, Poly-SNO-HSA or PEG-Poly-SNO-HSA at doses of 5 μmol NO/kg were injected as a bolus through the tail vein of 5-week-old male Donryu rats (200–250 g), and NO concentrations in plasma were determined at 1, 15, 30, 60, 180, and 360 min after injection. The amounts of the *S*-nitrosated moieties of Poly-SNO-HSA and PEG-Poly-SNO-HSA were quantified using a 96-well plate. First, 20 μL aliquots of Poly-SNO-HSA or

DOI 10.1002/jps.24020

Table 1. Pharmacokinetic Parameters for HSA and NO After Intravenous Administration (5 μmol/kg) of Poly-SNO-HSA to Normal Mice

	AUC_{0-4} (mM min)	CL_{tot} (mL/min/kg)	$t_{1/2\beta}$ (min)	V_1 (mL/kg)
HSA	52.10 ± 6.56	0.10 ± 0.05	476.6 ± 12.6	60.10 ± 4.35
NO moieties	11.17 ± 4.43	2.87 ± 0.75	118.7 ± 11.8	75.47 ± 6.54

All values are mean ± SD ($n = 5$).

PEG-Poly-SNO-HSA solution and $NaNO_2$ (standard) were incubated for 30 min at room temperature with 0.2 mL of 10 mM sodium acetate buffer (pH 5.5) containing 100 mM NaCl, 0.5 mM DTPA, 0.015% N-1-naphthylsthylene-diamide, and 0.15% sulfanilamide with or without 0.09 mM $HgCl_2$. Then, the absorbance was measured at 540 nm.[23]

Antitumor Study *In Vivo*

When tumors reached 150–200 mm^3, the mice were divided into cohorts (n = 4–5), and 200 μL saline (control); Poly-SNO-HSA (5 or 25 mg/mouse) or Poly-SNO-HSA dimer (0.5 or 2.5 mg/mouse) was injected via the tail vein three times per day on days 0, 2, and 4.[4] Afterwards, tumor volume and body weight were determined every day for 25 days. Tumor volume was calculated using the formula 0.4 ($a \times b^2$), where "a" is the largest and "b" is the smallest tumor diameter. After 25 days, blood samples were collected from the abdominal vena cava under anesthesia with diethylether of the mice that had received saline, Poly-SNO-HSA (25 mg/mouse), or Poly-SNO-HSA dimer (2.5 mg/mouse). Afterwards, the mice were sacrificed. Serum was isolated by centrifugation. Routine clinical laboratory techniques were used to determine the concentrations of total protein, serum creatinine (Cr), blood urea nitrogen (BUN), alanine aminotransferase (ALT), aspartate aminotransferase (AST), and alkaline phosphatase (ALP) in serum. Variance in each group was evaluated using the Bartlett test, and differences were evaluated using the Tukey–Kramer test.

Statistical Analysis

The statistical significance of collected data was evaluated using the ANOVA analysis followed by Newman–Keuls method for more than two means. Differences between the groups were evaluated by Student's t-test. $p < 0.05$ was regarded as statistically significant.

RESULTS AND DISCUSSION

Plasma Clearance of HSA and NO After Poly-SNO-HSA Administration

We determined the pharmacokinetic characteristics of both HSA and the NO moieties of Poly-SNO-HSA after its injection into normal male ddY mice (Table 1). As seen in Figure 1, the plasma concentration of the NO moieties decreases much more rapidly than that of HSA. In accordance with this finding, the half-life ($T_{1/2\beta}$) for HSA was calculated to be 477 min, whereas that for the NO moieties was only 119 min (Table 1). These data propose that the SNO stability of Poly-SNO-HSA is very low in the circulation.

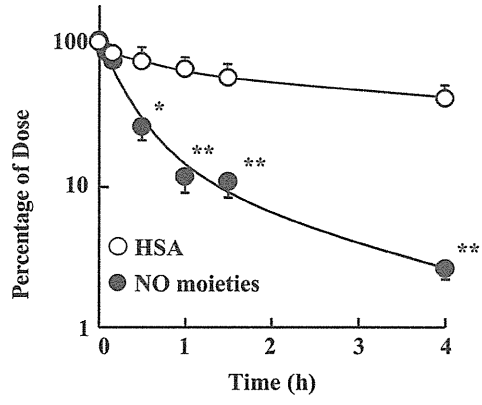

Figure 1. Plasma clearance of HSA and NO after intravenous administration (5 μmol/kg) of Poly-SNO-HSA to normal mice. Poly-SNO-HSA was injected as a bolus through the tail vein of mice, and HSA and NO concentrations in plasma are plotted against time after injection. Each datum point represents the mean ± SD. ($n = 5$). $^*p < 0.05$, $^{**}p < 0.01$ as compared with HSA.

In Vitro and *In Vivo* Release of NO from Poly-SNO-HSA and PEG-Poly-SNO-HSA

In an attempt to develop a more stable NO delivery system, we constructed pegylated Poly-SNO-HSA (PEG-Poly-SNO-HSA). First, we compared the stability of Poly-SNO-HSA and PEG-Poly-SNO-HSA in blood and plasma from normal mice at 37°C in the dark. Figure 2a shows that PEG-Poly-SNO-HSA is very stable as compared with Poly-SNO-HSA in blood. The half-life of PEG-Poly-SNO-HSA is 2.5 times longer than that of Poly-SNO-HSA. By contrast, there is no difference in stability between the two SNO preparations in plasma. The results suggest that *S*-denitrosation of Poly-SNO-HSA by other plasma proteins is insignificant and unaffected by pegylation.

For making an *in vivo* study of the NO release from Poly-SNO-HSA and PEG-Poly-SNO-HSA, we injected aliquots of the two protein preparations as a bolus through the tail vein of rats. As seen in Figure 2b, NO bound to the pegylated protein disappears more slowly from the circulation than does NO bound to the unpegylated protein; the NO half-lives are 155 and 105 min, respectively. Thus, both this study and that performed with mouse blood (Fig. 2a) shows that pegylation is a very useful way of SNO stabilization in the case of Poly-SNO-HSA.

Effect of Dimerization on the Antitumor Activity of Poly-SNO-HSA

One way of making cancer treatment more efficient is to increase the concentration of the therapeutic in the tumor. Such an increase in concentration can be obtained as the result of the EPR effect. For testing whether an increase in protein size would result in a more efficient EPR effect, we synthesized an albumin dimer that we also *S*-nitrosated, that is, Poly-SNO-HSA dimer. Figure 3a shows the antitumor activity of Poly-SNO-HSA dimer in mice compared with that of Poly-SNO-HSA. As seen, both albumin therapeutics have an inhibitory effect on tumor growth. However, Poly-SNO-HSA dimer possesses about at least 10 times higher antitumor activity than Poly-SNO-HSA.

In general, the body weights of the mice increased with reduction of tumor volume (Fig. 3b). An exception is the group of

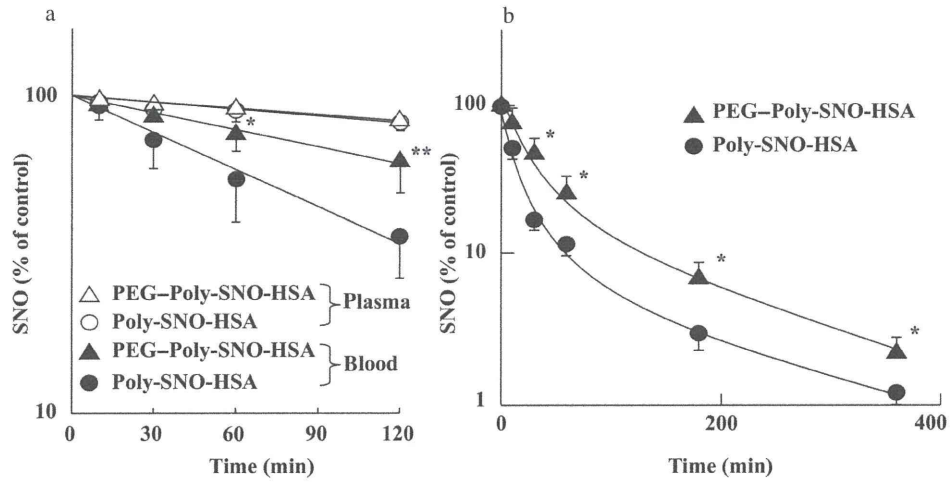

Figure 2. Time course for NO decay when incubated in blood or plasma (a) and plasma clearance of NO after intravenous administration of Poly-SNO-HSA or PEG-Poly-SNO-HSA (b). Poly-SNO-HSA or PEG-Poly-SNO-HSA at the concentration of 100 μM was incubated in mouse blood or plasma at 37°C for the indicated time in the dark. Each datum point represents the mean ± SD for three experiments. $^{*}p < 0.05$, $^{**}p < 0.01$ as compared with Poly-SNO-HSA in blood. Poly-SNO-HSA or PEG-Poly-SNO-HSA (5 μmol/kg) was injected as a bolus through the tail vein of rats, and NO concentrations in plasma are plotted against time after injection. $^{*}p < 0.05$ as compared with Poly-SNO-HSA.

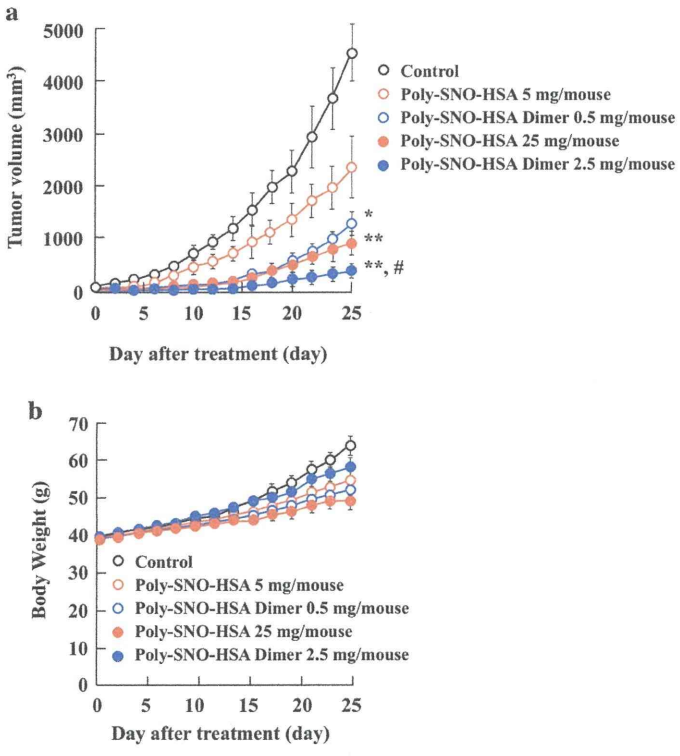

Figure 3. Effect of Poly-SNO-HSA and Poly-SNO-HSA dimer on tumor growth (a) and body weight (b) of C26 tumor-bearing mice. The C26 tumor-bearing mice were divided into cohorts ($n = 4$–5), and saline (control) or Poly-SNO-HSA (5 or 25 mg/mouse) or Poly-SNO-HSA dimer (0.5 or 2.5 mg/mouse) was injected three times per day on days 0, 2, and 4 via the tail vein. Results are for the following 25 days and are given as means ± SD. $^{*}p < 0.05$, $^{**}p < 0.01$ as compared with control. $^{\#}p < 0.05$ as compared with Poly-SNO-HSA (25 mg/mouse).

mice that each received 2.5 mg of Poly-SNO-HSA dimer. Their body weight increased more than expected, a finding suggesting that these mice may recover very well and fast from the hypophagia associated with the colon cancer.

Table 2 shows values of serum biochemical parameters of the C26 tumor-bearing mice treated with saline, Poly-SNO-HSA, or Poly-SNO-HSA dimer. As seen, total protein and serum creatinine (Cr) showed no significant differences among the three treated groups. However, BUN, AST, ALT, and ALP significantly decreased by Poly-SNO-HSA dimer treatment, indicating that Poly-SNO-HSA dimer did not cause hepatic or renal damage. In general, ALP levels increase in several types of cancer, such as liver, lung, and bone cancer, whereas the present finding indicates that Poly-SNO-HSA dimer protects against various organ damage induced by the tumor. Thus, the present findings suggest that Poly-SNO-HSA dimer is an effective and safe anticancer agent.

CONCLUSIONS

Previous studies have shown that Poly-SNO-HSA possesses antitumor activity *in vivo*. However, the SNO groups of Poly-SNO-HSA have low stability in the circulation, and high dosages of Poly-SNO-HSA cause reduction in the mean arterial blood pressure.[9] In this paper, we performed two tuning methods of Poly-SNO-HSA, namely, pegylation and dimerization. We found that pegylation enhances the stability of the *S*-nitrosated sites of Poly-SNO-HSA both *in vitro* and *in vivo*. Furthermore, dimerization of Poly-SNO-HSA resulted in improved antitumor activity via more efficient delivery of NO in C26 tumor-bearing mice. In addition, as an antitumor nanomedicine, PEG-Poly-SNO-HSA dimer possesses an important high biocompatibility and biodegradability. These findings lead to the idea that PEG-Poly-SNO-HSA dimer possesses the clinical possibility for being a superior and promising anticancer drug with reduction of side effects.

ACKNOWLEDGMENTS

This work was supported in part by grants-in-aid from the Japan Society for the Promotion of Science (JSPS), a

Table 2. Serum Biochemical Parameters of Control Mice and C26 Tumor-Bearing Mice Treated with Saline, Poly-SNO-HSA, or Poly-SNO-HSA Dimer

	Control Mice (Not Tumor-Bearing Mice)	Saline	Poly-SNO-HSA (25 mg/mouse)	Poly-SNO-HSA Dimer (2.5 mg/mouse)
Total protein (g/dL)	5.35 ± 0.35	5.23 ± 0.21	5.55 ± 0.24	5.32 ± 0.20
Cr (mg/dL)	0.10 ± 0.07	0.13 ± 0.04	0.16 ± 0.01	0.14 ± 0.01
BUN (mg/dL)	18.6 ± 2.76	15.25 ± 0.96	13.75 ± 1.26	12.45 ± 0.76*
AST (U/L)	67.7 ± 12.9	143.5 ± 62.9	116.3 ± 69.1	102.1 ± 63.7*
ALT (U/L)	39.7 ± 13.6	169.8 ± 111.6	161.3 ± 126.2	101.1 ± 108.7**,##
ALP (U/L)	329.1 ± 23.3	385.3 ± 18.3	300.5 ± 23.0**	276.5 ± 21.2**,#

All values are mean ± SD ($n = 4–5$).
*$p < 0.05$, **$p < 0.01$, versus saline; #$p < 0.05$, ##$p < 0.01$ versus Poly-SNO-HSA.

grant-in-aid from the Ministry of Education, Culture, Sports, Science and Technology (KAKENHI 25860118, 23390142, and 21390177), Japan. The work was also in part supported by grants from the Uehara Memorial Foundation and the Yasuda Medical Foundation.

REFERENCES

1. Ishima Y, Hara M, Kragh-Hansen U, Inoue A, Suenaga A, Kai T, Watanabe H, Otagiri M, Maruyama T. 2012. Elucidation of the therapeutic enhancer mechanism of poly-S-nitrosated human serum albumin against multidrug-resistant tumor in animal models. J Control Release 164:1–7.
2. Park K. 2012. Poly-SNO-HSA: A safe and effective multifunctional antitumor agent. J Control Release 164:105.
3. Moncada S, Palmer RM, Higgs EA. 1991. Nitric oxide: Physiology, pathophysiology, and pharmacology. Pharmacol Rev 43:109–142.
4. Katayama N, Nakajou K, Komori H, Uchida K, Yokoe J, Yasui N, Yamamoto H, Kai T, Sato M, Nakagawa T, Takeya M, Maruyama T, Otagiri M. 2008. Design and evaluation of S-nitrosolated human serum albumin as novel anticancer drug. J Pharmacol Exp Ther 325:69–76.
5. Ishima Y, Yoshida F, Kragh-Hansen U, Watanabe K, Katayama N, Nakajou K, Akaike T, Kai T, Maruyama T, Otagiri M. 2011. Cellular uptake mechanisms and responses to NO transferred from mono- and poly-S-nitrosated human serum albumin. Free Radic Res 45:1196–1206.
6. Ishima Y, Kragh-Hansen U, Maruyama T, Otagiri M. 2013. Poly-*S*-nitrosated albumin as a safe and effective multifunctional antitumor agent: Characterization, biochemistry and possible future therapeutic applications. Biomed Res Int 2013:353892.
7. Marley R, Feelisch M, Holt S, Moore K. 2000. A chemiluminescense-based assay for S-nitrosoalbumin and other plasma *S*-nitrosothiols. Free Radic Res 32:1–9.
8. Marks DS, Vita JA, Folts JD, Keaney JF Jr, Welch GN, Loscalzo J. 1995. Inhibition of neointimal proliferation in rabbits after vascular injury by a single treatment with a protein adduct of nitric oxide. J Clin Invest 96:2630–2638.
9. Katsumi H, Nishikawa M, Yamashita F, Hashida M. 2005. Development of polyethylene glycol-conjugated poly-*S*-nitrosated serum albumin, a novel *S*-Nitrosothiol for prolonged delivery of nitric oxide in the blood circulation in vivo. J Pharmacol Exp Ther 314:1117–1124.
10. Katayama N, Nakajou K, Ishima Y, Ikuta S, Yokoe J, Yoshida F, Suenaga A, Maruyama T, Kai T, Otagiri M. 2010. Nitrosylated human serum albumin (SNO-HSA) induces apoptosis in tumor cells. Nitric Oxide 22:259–265.
11. Shishido SM, de Oliveira MG. 2000. Polyethylene glycol matrix reduces the rates of photochemical and thermal release of nitric oxide from S-nitroso-N-acetylcysteine. Photochem Photobiol 71:273–280.
12. Maeda H, Sawa T, Konno T. 2001. Mechanism of tumor-targeted delivery of macromolecular drugs, including the EPR effect in solid tumor and clinical overview of the prototype polymeric drug SMANCS. J Control Release 74:47–61.
13. Maeda H, Wu J, Sawa T, Matsumura Y, Hori K. 2000. Tumor vascular permeability and the EPR effect in macromolecular therapeutics: A review. J Control Release 65:271–284.
14. Maeda H. 2001. SMANCS and polymer-conjugated macromolecular drugs: Advantages in cancer chemotherapy. Adv Drug Deliv Rev 46:169–185.
15. Yuan F, Leunig M, Huang SK, Berk DA, Papahadjopoulos D, Jain RK. 1994. Microvascular permeability and interstitial penetration of sterically stabilized (stealth) liposomes in a human tumor xenograft. Cancer Res 54:3352–3356.
16. Matsumura Y, Maeda H. 1986. A new concept for macromolecular therapeutics in cancer chemotherapy: Mechanism of tumoritropic accumulation of proteins and the antitumor agent SMANCS. Cancer Res 46:6387–6392.
17. Cabral H, Matsumoto Y, Mizuno K, Chen Q, Murakami M, Kimura M, Terada Y, Kano MR, Miyazono K, Uesaka M, Nishiyama N, Kataoka K. 2011. Accumulation of sub-100 nm polymeric micelles in poorly permeable tumours depends on size. Nat Nanotechnol 6:815–823.
18. Matsushita S, Chuang VT, Kanazawa M, Tanase S, Kawai K, Maruyama T, Suenaga A, Otagiri M. 2006. Recombinant human serum albumin dimer has high blood circulation activity and low vascular permeability in comparison with native human serum albumin. Pharm Res 23:882–891.
19. Chen RF. 1967. Removal of fatty acids from serum albumin by charcoal treatment. J Biol Chem 242:173–181.
20. Abuchowski A, van Es T, Palczuk NC, Davis FF. 1977. Alteration of immunological properties of bovine serum albumin by covalent attachment of polyethylene glycol. J Biol Chem 252:3578–3581.
21. Ishima Y, Sawa T, Kragh-Hansen U, Miyamoto Y, Matsushita S, Akaike T, Otagiri M. 2007. *S*-nitrosylation of human variant albumin Liprizzi (R410C) confers potent antibacterial and cytoprotective properties. J Pharmacol Exp Ther 320:969–977.
22. Yamaoka K, Tanigawara Y, Nakagawa T, Uno T. 1981. A pharmacokinetic analysis program (multi) for microcomputer. J Pharmacobiodyn 4:879–885.
23. Akaike T. 2000. Mechanisms of biological *S*-nitrosation and its measurement. Free Radic Res 33:461–469.

校正中

EPR 効果に基づくポリマー抗癌剤の腫瘍デリバリー

微小癌の検出・治療を目的としたセラノスティック薬剤の開発

中　村　秀　明[*1]・方　　軍[*2]・前　田　　浩[*3]

手術不能の早期気管支肺癌

1．はじめに

光照射により励起した光増感剤は，そのエネルギーを酸素分子に受け渡すことで，一重項酸素を発生する．一重項酸素は非常に反応性に富む活性酸素の一つであり，近傍の物質に酸化損傷を与える．そのため，光増感剤を癌組織に集積させた後に，癌組織に光を照射することで，その局所のみに一重項酸素を発生させ，癌組織選択的に酸化傷害を与えることが可能となり，癌治療を行うことができる．この癌治療法を光線力学的療法（PDT，photodynamic therapy）と呼び，わが国においては早期肺癌（0 期または 1 期）および腫瘍摘出手術施行時の原発性悪性脳腫瘍に対して承認されている．光増感剤としてはポルフィリン系の薬剤が最も知られており，2014 年現在，日本では，フォトフリン®（ポルフィマーナトリウム）およびレザフィリン®（タラポルフィンナトリウム）が，癌の光線力学的療法剤として認可，使用されている．しかし，投与後 2 週間は直射日光を避けるなど，光線過敏症を予防する措置が取られているのが現状であり，この問題はフォトフリンおよびレザフィリンなどの薬物動態の悪さに起因するところが多い．つまり，薬剤が皮膚へ分布するため，直射日光などにより紅斑，水泡等の光線過敏反応を引き起こす恐れがあり，改善が望まれている．

[*1] Hideaki Nakamura　崇城大学DDS研究所　薬学部微生物学研究室　助教　博士（薬学）
[*2] Jun Fang　同上　准教授　博士（医学）
[*3] Hiroshi Maeda　崇城大学DDS研究所　特任教授　博士（医学）
Micelles of Zinc Protoporphyrin Conjugated to HPMA Polymer for Imaging and Light-induced Antitumor Effect Based on the EPR Effect Driven Tumor Delivery

これら低分子薬剤である

考え

全身、とくに

癌組織で

ドラッグデリバリーサイエンス（DDS）研究は，薬物の体内動態の把握やメカニズムの解析，さらにその改善を目的とした研究であり，薬物そのものの改変によって，その動態に起因する問題を解決する研究分野である．例えば，癌治療における DDS の第一問題としては，松村・前田等の提唱した enhanced permeability and retention（EPR）効果の問題が挙げられる[1]．つまり，血中に投与された薬物が，組織への漏出性の亢進，ならびにリンパ系の機能不全による組織からの排除不全によって，より癌組織に持続的に滞留することができる．ただしその薬物は高分子型の抗癌剤（＞40 kDa）であることが必要である．つまり，癌組織に選択的に薬物が集積する現象が EPR 効果であり，それを利用したものである．光増感剤も高分子化すればEPR 効果により，皮膚などの正常組織への分布が抑制され，癌組織に選択的に集積する．そのため，光線過敏症などの副作用の軽減のみならず，組織傷害の腫瘍選択性など治療効果の増強につながる．また，ポルフィリン系化合物を代表とする光増感剤の多くは，光照射により一重項酸素と蛍光を効率よく発する性質を持つため，癌組織に高濃度に集積させることで，蛍光を利用した癌組織の検出につなげること

腫瘍選択的な組織傷害となり

手法

応用

癌

選択的にかつ

とき用いる

ある．

同様に

が可能となる．つまり，EPR 効果を利用した DDS 製剤の技術を用いて，光増感剤を腫瘍に集積させ，副作用を軽減させ，治療効果の増大をはかり，癌組織の高感度検出という，全く新しい性質を持つ光線力学的療法剤の開発が可能になる．

2．高分子型光線力学的療法剤について

2．1　亜鉛プロトポルフィリン(ZnPP)

われわれの研究室では以前より，光増感剤として亜鉛プロトポルフィリン(ZnPP)を用いた高分子抗癌剤の研究を行ってきた[2~8]．ZnPP はプロトポルフィリン IX に亜鉛が配位した構造を持つ．ZnPP は光増感剤として機能するのみならず，ヘム酸化酵素(heme oxygenase，HO-1)の阻害剤としても知られる[9]．ヘム酸化酵素は多くの癌細胞において発現亢進が見られる抗酸化酵素であり，HO-1 の機能阻害により，酸化ストレスへの抵抗力を減弱させれば，癌細胞は酸化傷害を受けアポトーシスに至る[10]．つまり，ZnPP は癌の酸化防御機構を抑制するとともに，光により一重項酸素を発生することで強力に癌細胞に対して酸化傷害を引き起こす．これに対する問題は，ZnPP の水溶性が極めて低いこと，ならびに他の光増感剤と同様に癌組織への集積性が悪いために，治療薬としては難があった．そこでわれわれは DDS 技術を用いた ZnPP の水溶化と癌組織への集積性の向上を図る必要を認めた．

2．2　高分子型亜鉛プロトポルフィリン

ZnPP の問題点に対し，われわれはこれまでにスチレンマレイン酸コポリマー(SMA)またはポリエチレングリコール(PEG)を用い高分子化により，EPR 効果を利用した，腫瘍標的型水溶性 ZnPP 製剤を作製し，その有用性を明らかにしてきた[7,8]．しかし，ZnPP そのものは正常細胞への毒性はほとんどないとはいえ，腫瘍集積性に加え肝臓や脾臓への

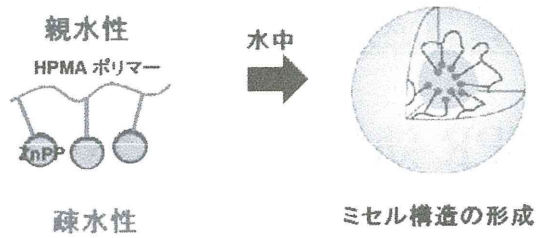

図 1　HPMA-ZnPP の模式図

集積も高く，ZnPP 含有率の低さなどに問題が認められた．その延長線上の研究成果としてわれわれはヒドロキシプロピルメタアクリルアミドポリマー(PHPMA)を用いた高分子 ZnPP 製剤が有用であることを見出した．つまり，PHPMA の側鎖のヒドロキシル基に ZnPP のカルボキシル基を結合した HPMA-ZnPP の作製を行った(図 1)．この HPMA-ZnPP は水中でミセル構造を形成し，高分子化合物として挙動する．さらに ZnPP の含有率を 30%程度まで上げることが可能となり，高い水溶性と腫瘍集積性を合わせ持つ DDS 製剤である．

2．3　光照射による細胞傷害性の獲得

一般に ZnPP などのテトラピロール化合物の光増感作用はよく知られている性質であり，われわれは ZnPP に対して光を照射することで，一重項酸素を発生し，細胞傷害性が大幅に向上することをこれまでに明らかにしてきている．当然のことながら HPMA-ZnPP も光増感作用を有しており，光照射により一重項酸素を発生することを電子スピン共鳴装置(ESR)により確認している(図 2 A，B)．また，一重項酸素の発生は界面活性剤の存在下において顕著に見られ，図 2 B では界面活性剤である Tween 20 存在下において一重項酸素の発生が促進することを示している．さらにわれわれは細胞膜成分であるレシチンも同様の作用を示すことを未発表ではあるが明らかにしており，HPMA-ZnPP が細胞に取り込まれる際に，レシチンの作用により HPMA-ZnPP は一重項酸素を放出できる構造になる

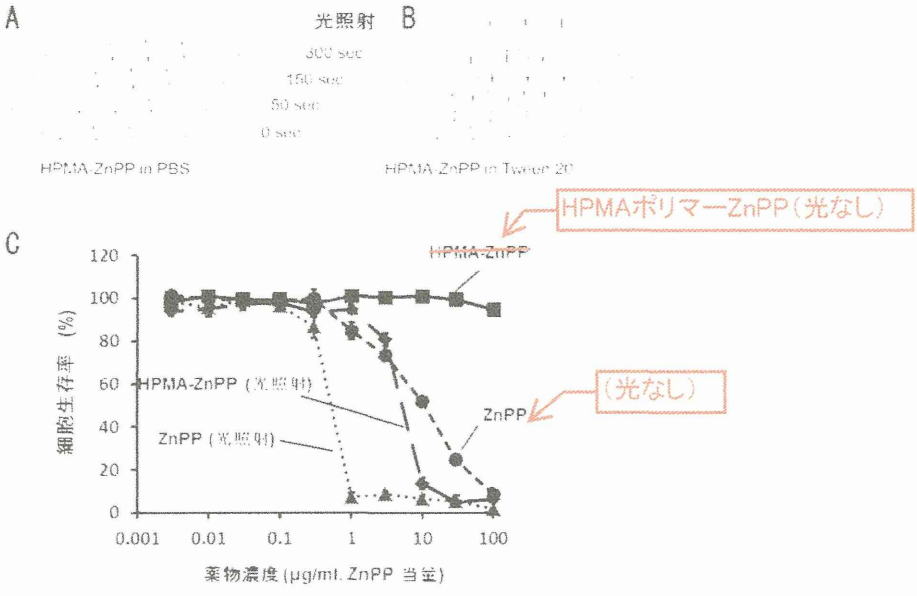

図２　HPMA-ZnPP による一重項酸素の発生と生物活性の増強
光照射による一重項酸素の生成量を PBS（A）または界面活性剤（B）中において，電子スピン共鳴（ESR）装置を用いて測定した．（C）HeLa 細胞に HPMA-ZnPP または ZnPP を処理し，光を照射した後に細胞生存率を測定した

ことを示唆している．実際に癌細胞に対して HPMA-ZnPP を処理し，光を照射することで，細胞傷害性の大幅な増大が見られ，HPMA-ZnPP が光増感作用を示すことを明らかにした（図２B）．

ポリマー

2．4　HPMA-ZnPP の薬物動態と光イメージング

HPMA-ZnPP は生体内における薬物動態の改善を目的とした薬剤であり，ZnPP と比較して，大幅な腫瘍集積性の向上と正常組織への分布の抑制が認められる[1]．HPMA-ZnPP が，癌組織に高濃度に集積すること，また光照射により蛍光を発する性質を利用し，癌組織の蛍光イメージングが可能であるかを検討した．S180 担癌マウスに HPMA-ZnPP を投与し，*in vivo* 蛍光イメージング装置（IVIS lumina XR）を用い，蛍光イメージングを行ったところ，癌組織選択的に蛍光が観察された（図３A）．さらに，蛍光フィルターを用いることで，市販のコンパクトカメラでも同様に癌組織の蛍光イメージングが可能であることを明らかにしている（図３B）．この結果は，

マウスそのままで

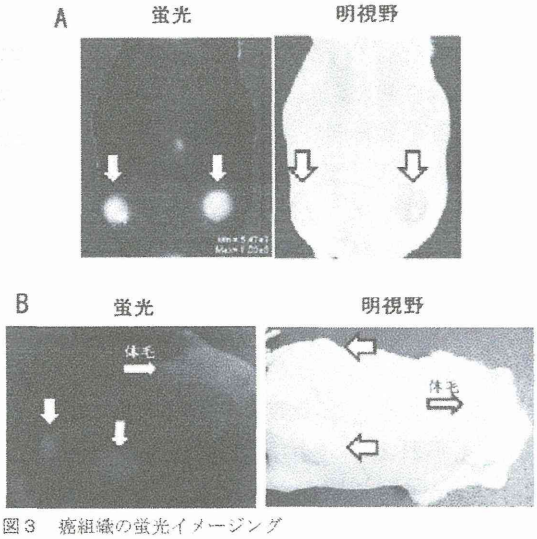

図３　癌組織の蛍光イメージング
S180 担癌マウスに HPMA-ZnPP を投与し，in vivo 蛍光イメージング装置（IVIS Lumina-XR）（A），または市販のコンパクトカメラ（B）を用いて，腫瘍の画像可視化（蛍光イメージング）を行った．矢印は移植癌を示す．体毛部に非特異的な自家蛍光が認められる

の

内視鏡や腹腔鏡などの一般的な光学機器を用いた体腔内（腹膜，胸壁，肝皮膜，内膀胱，子宮など）癌組織の蛍光検出に応用可能であることを示唆している．リアルタイムな癌組織の蛍光観察が可能になれば，目視では判断

の検出と、それ　の

し難い，微小癌に対する光線力学的療法施術時において光照射部位を決定する際に有用な情報を提供することが可能となる．

を効率的に行うことができる。

2．5　HPMA-ZnPP による抗癌効果

In vitro における HPMA-ZnPP の光増感作用に関しては，前記（図３）の光による細胞毒性（殺細胞作用の増強）は，100 μg/ml で無毒のものが，10 μg/ml 以下で 50％の細胞を殺傷するようになる．また，体内動態の改善も認められ，蛍光イメージングにおいても，容易に HPMA-ZnPP が癌組織へ選択的に集積していることが確認された．これまでに，S180 マウス移植癌モデルに対して HPMA-ZnPP の抗癌効果も確認してきた[11]．さらに，ラット化学発癌モデルに関して HPMA-ZnPP の抗腫瘍効果の検討を行ったところ，同様の結果が得られた．この実験モデルにおいては SD ラットにジメチルベンズアントラセン（DMBA）を経口投与することにより，乳腺癌を形成させた．このモデルは移植癌とは異なり，自家発癌モデルであるため，より本物の癌に近いモデルである．HPMA-ZnPP を投与後に，キセノン光を用いて光照射を行ったところ，HPMA-ZnPP 1 回投与，光照射 2 回で，乳腺癌の消失が確認された（図４）．しかし，HPMA-ZnPP 単独（光照射なし）では治療効果が見られなかったことから，治療効果は光照射による一重項酸素生成に起因するものと考えられる．本治療においては，高価なレーザー照射装置などを必要とせず，安価なキセノン光ないしは LED 光で十分な効果が期待できる．また，このモデルにおいても HPMA-ZnPP による蛍光イメージングは可能であった（未発表データ）．

ま と め

手術を必要としない，非侵襲的な癌治療法である光線力学的療法は，癌患者にとって優しい治療法である．しかし，既存の光線力学的療法剤は薬物動態が悪いため，副作用が大

ポリマー　の同定

きな問題となってきた．われわれの作製した HPMA-ZnPP は，癌組織に選択的に集積するため，副作用の問題は解決できると考えられる．さらに，癌の蛍光イメージングが可能であり，癌組織の場所さらには薬剤が集積しているか否かの判断が非常に容易になっている．そのため，光を照射すべき部位が容易に判断でき，効率的な施術が可能となると考えられる．現在は内視鏡や腹腔鏡を用いた光線力学的治療や，癌組織の検出への応用・導出を目指して検討を行っている．

どの程度

ポリマー　研究

1）Matsumura, Y. and H. Maeda, A new concept for macromolecular therapeutics in cancer chemotherapy: mechanism of tumoritropic accumulation of proteins and the antitumor agent smancs. *Cancer Res*, 1986. **46**(12 Pt 1): p. 6387-92.

2）Fang, J., *et al.*, HSP32 (HO-1) inhibitor, copoly(styrene-maleic acid)-zinc protoporphyrin IX, a water-soluble micelle as anticancer agent: In vitro and in vivo anticancer effect. *Eur J Pharm Biopharm*, 2012. **81**(3): p. 540-7.

3）Herrmann, H., *et al.*, The Hsp32 inhibitors SMA-ZnPP and PEG-ZnPP exert major growth-inhibitory effects on D34+/CD38+ and CD34+/CD38- AML progenitor cells. *Curr Cancer Drug Targets*, 2012. **12**(1): p. 51-63.

4）Gleixner, K.V., *et al.*, Targeting of Hsp32 in solid tumors and leukemias: a novel approach to optimize anticancer therapy. *Curr Cancer Drug Targets*, 2009. **9**(5): p. 675-89.

5）Iyer, A.K., *et al.*, Polymeric micelles of zinc protoporphyrin for tumor targeted delivery based on EPR effect and singlet oxygen generation. *J Drug Target*, 2007. **15**(7-8): p. 496-506.

6）Regehly, M., *et al.*, Water-soluble polymer conjugates of ZnPP for photodynamic tumor therapy. Bioconjug Chem, 2007. 18(2): p. 494-9.

7）Iyer, A.K., *et al.*, High-loading nanosized micelles of copoly(styrene-maleic acid)-zinc protoporphyrin for targeted delivery of a potent heme oxygenase inhibitor. *Biomaterials*, 2007. **28**(10): p. 1871-81.

8）Sahoo, S.K., *et al.*, Pegylated zinc protoporphyrin: a water-soluble heme oxygenase inhibitor with tumor-targeting capacity. *Bioconjug Chem*, 2002. **13**(5): p. 1031-8.

9）Maines, M.D., Zinc . protoporphyrin is a selective inhibitor of heme oxygenase activity in the neonatal rat. *Biochim Biophys Acta*, 1981. **673**(3): p. 339-50.

10）Fang, J., T. Akaike, and H. Maeda, Antiapoptotic role of heme oxygenase (HO) and the potential of HO as a target in anticancer treatment. *Apoptosis*, 2004. **9**(1): p. 27-35.

11）Nakamura, H., *et al.*, Micelles of zinc protoporphyrin conjugated to N-(2-hydroxypropyl)methacrylamide (HPMA) copolymer for imaging and light-induced antitumor effects in vivo. *J Control Release*, 2013. **165**(3): p. 191-8.

Research Article

For J Pharm Sci (*Pharmaceutical Nanotechnology*)

Enhanced bacterial tumor delivery by modulating the EPR effect, and therapeutic potential of *Lactobacillus casei*

Jun Fang[1,2], Long Liao[1,3], Hongzhuan Yin[1], Hideaki Namamura[1,2], Takashi Shin[3], Hiroshi Maeda[1]

[1]*Institute of Drug Delivery Science,* [2]*Laboratory of Microbiology and Oncology, Faculty of Pharmaceutical Sciences, and* [3]*Department of Applied Microbial Technology, Faculty of Biotechnology and Life Science, Sojo University, Ikeda 4-22-1, Kumamoto 860-0082, Japan.*

Corresponding Author: Hiroshi Maeda, or Jun Fang, DDS Research Institute, Sojo University, Kumamoto 860-0082, Japan. Phone: +81-96-326-4114; Fax: +81-96-326-3158; E-mail: hirmaeda@ph.sojo-u.ac.jp (HM)., fangjun@ph.sojo-u.ac.jp (JF).

Running title: Enhanced bacterial therapeutic effect by modulating EPR effect

Abbreviations: EPR effect, enhanced permeability and retention effect; *L. casei, Lactobacillus casei*; NG, nitroglycerin; NO, nitric oxide; ACE, angiotensin II converting enzyme.

Abstract

Bacteria of micrometer size could accumulate in tumor based on EPR effect. We report here *Lactobacillus casei (L. casei)*, a nonpathogenic facultatively anaerobic bacterium, preferentially accumulated in tumor tissues after intravenously (i.v.) injection; at 24h, live bacteria were found more in the tumor, whereas the bacteria in normal tissues including the liver and spleen were cleared rapidly. The tumor-selective accumulation and growth of *L. casei* is probably due to the EPR effect and the hypoxic tumor environment. Moreover, the bacterial tumor delivery was significantly increased by a NO donor nitroglycerin (NG, 10-70 times) and an angiotensin II converting enzyme inhibitor, enalapril (6-18 times). Consequently significant suppression of tumor growth was found in a colon cancer C26 model, and more remarkable antitumor effect was achieved when *L. casei* was combined with NG, probably by modulating the host nonspecific immune responses; tumor necrosis factor-α significantly increased in tumor after the treatment, as well as NO synthase activity and myleoperoxidase activity. These findings suggest the potential of *L. casei* as a candidate for targeted bacterial antitumor therapy, especially in combine with NG or other vascular mediators.

Keywords: EPR effect, *Lactobacillus casei*, Nitroglycerin, vascular permeability, ACE inhibitor

INTRODUCTION

Historical experience using bacteria for the therapeutic purpose against cancer goes back to the end of 19 century pioneered by Wiliam Coley, later called Coley's toxin or Coley's vaccine,[1,2] in which *Sereptococcus pyogenes* and *Serratia marcescens* were injected into tumor directly. In the recent decade bacterial therapy as a new anticancer strategy is gaining more attention than ever through systemic administration of bacteria.

Hoffman et al.[3,4] reported that intravenous injection of a modified strain of *Salmonella typhimurium* selectively infected tumor tissues and induced significant tumor shrinkage in many tumor models in mice. Taniguchi's group developed tumor-targeted delivery of genetically engineered *Bifidobacterium longum* expressing cytosine deaminase as a prodrug that would trigger the generation of 5-fluorouracil in tumor, resulting in remarkable antitumor effects.[5] Both of these methods are now in clinical trials. Also, by using *Escherichia coli* or *Salmonella enterica serovar Typhimurium* Xiang et al. successfully developed a tumor-targeted delivery system of short hairpin RNA.[6] In addition, recently many reports have indicated that *Lactobacillus casei (L. casei)*, a nonpathogenic bacterium widely used in dairy products, exhibits antitumor therapeutic potential by enhancing the cellular immunity of the host.[7,8] All these results suggest that bacterial therapy is a promising approach in cancer treatment, and thus, it is intriguing to analyze bacterial accumulation and growth in tumor tissues.

Regarding the tumor accumulation of bacteria, anaerobic or facultative bacteria have been known for decades to grow selectively in tumors.[3-5, 9-11] This growth is now attributed to the unique pathophysiological features found in many tumors, i.e., impaired and abnormal vascular architecture, high vascular permeability and hypoxia, or low pO_2, together with extensive necrosis.[3-5, 12] In this context, we have been working on tumor selective drug delivery and found that macromolecules above 40 kDa effectively traverse tumor blood vessels permitting their accumulation in tumor tissues.[13-15] This unique phenomenon of biocompatible macromolecules in solid tumor was coined enhanced permeability and retention (EPR) effect, which is attributed to the defective architecture of neovasculature of tumor, as well as various vascular mediators such as nitric oxide (NO) and bradykinin that facilitates opening of endothelial cell-cell gaps.[12,15,16] We also found the EPR effect occurs even in macromolecules beyond 10^6 Da or nanoparticles as large as 1000 nm, the size of bacteria.[12] More recently we found that the EPR effect could be further augmented by applying nitroglycerin (NG) which becomes NO in hypoxic milieu of tumor, and angiotensin I converting enzyme (ACE) inhibitor that suppresses degradation of bradykinin (kinin) thereby resulting in higher kinin content in tumor.[12,17,18]

In view of these findings, it is strongly indicated that delivery of bacteria to tumor and thus bacterial therapeutic could be further enhanced by modulating vascular mediators, i.e., NO and bradykinin. We thus examined, in the present study, whether tumor selective delivery of bacteria can be increased by applying NG and ACE inhibitor (enalapril) both of which are commonly used clinically to cause vascular dilatation or antihypertension.

MATERIALS AND METHODS

Materials

NG ointment (Vasolator®) containing 20 mg of NG/g Vaseline®, was from Sanwa Kagaku Kenkyusho (Nagoya, Japan) and was used after 10- or 100-fold dilution with Vaseline®. Enalapril was purchased from Elmed Eisai Co., Ltd. (Tokyo, Japan). NO donor 1-Hydroxy-2-oxo-3-(*N*-methyl-3-aminopropyl)-3-methyl-1-triazene (NOC7) was from Dojindo Laboratories (Kumamoto, Japan). Other chemicals of reagent grade were from Wako Pure Chemical Industries (Osaka, Japan) and were used without further purification.

Bacteria and cells

L. casei strain *Shirota* was kindly from Yakult Honsha Co., Ltd. (Tokyo, Japan) and was cultured in MRS (de Man, Rogosa, Sharpe) medium (Cica; Kanto Chemical Co. Inc., Tokyo, Japan). Lactulose (4-O- β -D -galactopyranosyl-D-fructofuranose, Wako Pure Chemical Industries) was used during in vivo experiments with *L. casei*.

Mouse S-180 sarcoma cells were maintained in ascites of ddY mouse by weekly passage. Colon cancer C26 cells were kindly gift from Dr. Ishima of Kumamoto University (Japan), and were maintained and cultured in RPMI-1640 medium (Invitrogen, Carlsbad, CA) at 37°C in an atmosphere of 5% CO_2/95% air

Animal solid tumor models

Male ddY mice of 6 weeks old and female BALB/c mice (6 weeks old) were obtained from Kyudo Inc. (Saga, Japan). All animals were maintained under standard conditions: a 12-h dark/light cycle and a temperature of 23 ± 1°C. Mice were fed water and murine chow *ad libitum*. All experiments were carried out according to the guidelines of the Laboratory Protocol of Animal Handling, Faculty of Pharmaceutical Sciences, Sojo University.

Mouse S-180 sarcoma cells (2×10^6) were implanted subcutaneously (s.c.) in the dorsal skin of ddY mice, to obtain the S-180 tumor model in mice, and cultured colon adenocarcinoma C26 cells were implanted s.c. in the dorsal skin of BALB/c mice as C26 solid tumor model. At 10-15 days after implantation of tumor cells, when the tumors became 8-10 mm in diameter, the following studies were carried out.

Body distribution of L. casei in murine solid tumor with and without NG or enalapril treatment

To investigate the biodistribution of *L. casei*, bacteria (7×10^6 CFU, in 0.1 ml culture medium) were injected i.v. via the tail vein in S-180 or C26 mouse solid tumor model, followed by i.p. injection of 1 ml of 20% lactulose. For the NG-treated group, NG ointment (at NG dose of 0.6 mg/tumor) was applied to the skin over the tumors 5 min before the injection of bacteria. For enalapril-treated group, enalapril (10 mg/kg) was given orally 4 h before the injection of bacteria.

At scheduled times (i.e., 1, 6, 24, 48h) after the injection of bacteria, mice were killed and blood was collected from the inferior vena cava, and mice were then subjected to reperfusion with 10 ml of physiological saline containing 5 U/ml heparin to remove blood components from the blood vessels of various organs and tissues. Tumor tissues and normal organs and tissues, including the liver, spleen, kidney, heart, and lung, were collected and weighed. To each tissue, 9-time volume of cold physiological saline was added, and then tissues were minced and homogenized on ice with Polytron homogenizer (Kinematica, Littau-Lucerne, Switzerland). Tissue homogenates (50 μl) at different dilutions were transferred to 10 cm Petri dishes, and then 15 ml of MRS agar medium kept at 40°C was added and thoroughly mixed. The dishes were then placed at room temperature to solidify the agar medium, after which they were placed in an incubator at 37°C. After 2 days of incubation, *L. casei* colonies were counted. The distribution of bacteria in each tissue was expressed as CFU/g tissue or CFU/ml blood. All experiments were performed duplicate under sterilized conditions.

In vivo therapeutic effect of L. casei by i.v. injection and its enhancement by NG

The therapeutic effect of *L. casei* was investigated in the C26 solid tumor model. Ten days after injection of C26 tumor cells in BALB/c mice, when tumor diameters became 5-8 mm, *L casei* (7×10^6 CFU or 2×10^7 CFU) was injected i.v.; in some experiments, NG ointment (at an NG dose of 0.6 mg/ tumor) was rubbed on the skin overlying the tumors just before administration of bacteria. This therapeutic protocol was carried out once a week for 3 weeks. During the period of experiments, 1 ml of 20% lactulose was i.p. injected daily till 2 days after the last injection of *L. casei.* Tumor volume and body weight of animals were measured, and tumor volume was estimated by measuring longitudinal cross section (L) and transverse section (W) and applying the formula $V = (L \times W^2)/2$.

Measurement of myeloperoxidase (MPO) and NO synthase (NOS) activity in tumor after L. casei treatment with/without NG

In S-180 solid tumor model, the MPO activity and iNOS activity in tumor after *L. casei* with/without NG were measured by using the colorimetric MPO activity assay kit (BioVision Inc., Milpitas, CA) and a colorimetric NOS assay kit (Oxford Biomedical Research, Inc.,

Oxford, MI) respectively, according to the manufacturers instructions. In this experiment, NG and/or *L. casei* (2×10^7 CFU) were administered by the protocol as described above but applied once every two days, and 1 ml of 20% lactulose was given i.p. daily. Four days after the last injection of bacteria, mice were killed and tumor tissues were collected for the assays.

Enzyme-linked immunosorbent assay (ELISA) for interleukin-6 (IL-6) and tumor necrosis factor (TNFα) in serum and tumor of S-180 tumor bearing mice after L. casei treatment with/without NG.

By the same protocol for measurement of MPO and NOS activity, quantifications of cytokines IL-6 and TNFα were performed. Namely, serum and tumor tissues from S-180 tumor bearing mice with each treatment were subjected to ELISA (ELISA kits, R&D Systems, Inc., Minneapolis, MN) according to the manufacturer's instructions.

Effect of sodium nitrite and NOC7 on the growth of L. casei

To investigate the potential effect of nitrite and NO on the growth of *L. casei*, in vitro experiments were carried out using cultured *L. casei*. Namely, *L. casei* was first cultured in MRS agar medium. After 24 h of culture at 37°C, a speck of bacteria was taken from a colony was put into 10 ml of MRS liquid medium and cultured at 37°C with shaking (120 rpm). After overnight incubation, 10 μl of cultured bacteria was transferred into 50 ml of MRS medium, in which different concentrations of sodium nitrite or NO donor NOC7 were added, and the bacteria were cultured continued under the same conditions. The bacterial growth was measured by absorbance at 600 nm every 30 min.

Statistical analysis

All data are expressed as means ± SD. Data were analyzed by one-way analysis of variance followed by the Bonferronit-test. Some studies with two experiments were analyzed by Mann–Whitney U-test, and a Fisher's exact test was used to analyze the data of survival rate. A difference was considered statistically significant when $P < 0.05$.

RESULTS

Body distribution of L. casei in tumor-bearing mice after i.v. injection

At 1h after i.v. injection of *L. casei* in S-180 tumor-bearing mice, most bacteria were found in liver and spleen (Fig. 1A). However, bacterial counts in normal tissues (e.g., liver and spleen) at 6h after injection significantly decreased to about 1/10 of those at 1 h, whereas the numbers of bacteria in the tumor significantly increased; it increased about 80 times (Fig. 1B). And at 24h, almost no living bacteria could be detected in normal tissues including liver and spleen (Fig. 1C), whereas, the bacteria in tumor have increased gradually with time; namely at 24h the bacteria in tumor were significantly higher (more than 50 times) than those in normal